Materials Science and Engineering C 59 (2016) 228–234

Contents lists available at ScienceDirect

Materials Science and Engineering C

journal homepage: www.elsevier.com/locate/msec

# Synthesis of flexirubin-mediated silver nanoparticles using *Chryseobacterium artocarpi* CECT 8497 and investigation of its anticancer activity

Chidambaram Kulandaisamy Venil [a], Palanivel Sathishkumar [b], Mahalingam Malathi [c], Rajamanickam Usha [d], Rajarajeswaran Jayakumar [e], Abdull Rahim Mohd Yusoff [b], Wan Azlina Ahmad [a,*]

[a] Department of Chemistry, Faculty of Science, Universiti Teknologi Malaysia, 81310 Skudai, Johor Bahru, Malaysia
[b] Centre for Environmental Sustainability and Water Security (IPASA), Research Institute for Sustainable Environment (RISE), Universiti Teknologi Malaysia, 81310 Skudai, Johor Bahru, Malaysia
[c] Department of Chemistry, Bannari Amman Institute of Technology, Sathyamangalam 638 401, Tamil Nadu, India
[d] Department of Microbiology, Karpagam University, Coimbatore 641 023, Tamil Nadu, India
[e] Department of Molecular Medicine, Faculty of Medicine, University of Malaya, 50603 Kuala Lumpur, Malaysia

ARTICLE INFO

*Article history:*
Received 9 May 2015
Received in revised form 4 October 2015
Accepted 7 October 2015
Available online 9 October 2015

*Keywords:*
Flexirubin
*Chryseobacterium*
Silver nanoparticles
Human breast cancer cells
Anticancer activity

ABSTRACT

In this work, the synthesis of silver nanoparticles from a pigment produced by a recently-discovered bacterium, *Chryseobacterium artocarpi* CECT 8497, was achieved, followed by an investigation of its anticancer properties. The bacterial pigment was identified as flexirubin following NMR ($^{1}$H NMR and $^{13}$C NMR), UV–Vis, and LC–MS analysis. An aqueous silver nitrate solution was treated with isolated flexirubin to produce silver nanoparticles. The synthesised silver nanoparticles were subsequently characterised by UV–Vis spectroscopy, Scanning Electron Microscopy (SEM), Energy Dispersive X-ray Spectroscopy (EDX), X-Ray Diffraction (XRD), and Fourier Transform Infrared (FTIR) Spectroscopy methodologies. Furthermore, the anticancer effects of synthesised silver nanoparticles in a human breast cancer cell line (MCF-7) were evaluated. The tests showed significant cytotoxicity activity of the silver nanoparticles in the cultured cells, with an IC50 value of 36 μg mL$^{-1}$. This study demonstrates that silver nanoparticles, synthesised from flexirubin from *C. artocarpi* CECT 8497, may have potential as a novel chemotherapeutic agent.

© 2015 Elsevier B.V. All rights reserved.

## 1. Introduction

Nanotechnology, an established applied science at the forefront of multi-disciplinary advancement, currently attracts significant attention with promising applications in diverse fields such as material science, nanomedicine, molecular nanoscience and chemistry. With numerous methodologies available for the synthesis of nanoparticles of particular shape and size according to specific requirements, notable developments are currently taking place in this technological field [1]. Nanoparticles (particles up to 100 nm in size) display completely new or improved properties when compared to larger particles [2], and provide solutions to various environmental and technological challenges. Metallic nanoparticles are considered the most promising as they exhibit positive antibacterial properties as a consequence of their large surface-area-to-volume ratio [3].

Among diverse metals, silver in its various forms has been widely used as a medicine for the treatment of a spectrum of diseases since ancient times [4]. Also known for its inhibitory effects on microbes in both medical treatments and industrial processes [5], the anti-microbial properties of silver are intensified following its transformation into a nanoparticle, rendering it useful in effectively eliminating fungus and bacteria [6]. As a natural material, silver is considered safe to man and produces few allergic reactions during clinical testing [7]. Silver nanoparticles have garnered attention due to their applicability in diverse areas such as catalysis, nanomedicine, biological labelling, solar cell surfaces, as staining pigments for glasses and ceramics, and as antimicrobial agents [4]. Apart from their antimicrobial properties, silver nanoparticles have been shown to have potential as anticancer agents due to their selective role in disrupting the mitochondrial respiratory chain which leads to the production of reactive oxygen species (ROS) and interruption of adenosine triphosphate (ATP) synthesis, thus causing nucleic acid damage [8,9].

Currently, a growing need exists to develop environmentally-benign processes for nanoparticle synthesis that do not employ toxic chemicals [10]. Incidentally, the advancement of 'green' chemistry to effectively synthesise silver nanoparticles using compounds derived from microbes has drawn remarkable attention in recent years [11]. Several studies have been undertaken to evaluate the synthesis of silver nanoparticles using compounds from a range of microbes as, compared with other physicochemical methods, the environmental issues

* Corresponding author.
*E-mail addresses:* ckvenil@gmail.com (C.K. Venil), azlina@kimia.fs.utm.my (W.A. Ahmad).

http://dx.doi.org/10.1016/j.msec.2015.10.019
0928-4931/© 2015 Elsevier B.V. All rights reserved.

associated with green chemistry technology are few. Furthermore, microbes appear to be the best candidates for the synthesis of nanoparticles on a large scale [12].

Amid diversified microbial compounds, flexirubin-type pigments (FTPs) from *Flavobacterium* sp. are capable of inhibiting the growth of *Mycobacterium* sp. and are thus applied in the treatment and prevention of tuberculosis [13]. Furthermore, Bej [13] confirms that FTPs exhibit anticancer and antimicrobial properties and can be considered as novel therapies for the treatment and prevention of cancer and microbial-mediated diseases, demands for which are increasing [14]. These properties of FTPs have generated interest in studying the anticancer properties of synthesised silver nanoparticles using FTPs derived from *Chryseobacterium* sp.

The present study aimed to assess the anticancer activity of silver nanoparticles in a human breast cancer cell line, following an evaluation of the synthesis of silver nanoparticles using flexirubin from *Chryseobacterium artocarpi* CECT 8497. To the best of our knowledge, this report is the first description of the synthesis of silver nanoparticles using flexirubin from *Chryseobacterium* sp. and subsequent evaluation of their anticancer properties.

## 2. Materials and methods

### 2.1. Chemicals

Nutrient broth, silver nitrate ($AgNO_3$), penicillin, streptomycin, L-glutamine, Dulbecco's modified Eagle medium (DMEM), dimethyl sulfoxide (DMSO), potassium bromide (KBr), and propidium iodide (PI) were purchased from Sigma-Aldrich, Malaysia and all analytical grade reagents used in this study were purchased from Merck, Malaysia.

### 2.2. Identification of Chryseobacterium sp.

Yellowish-orange pigment-producing bacteria isolated from the rhizosphere soil of *Artocarpus integer* from an orchard at Universiti Teknologi Malaysia (UTM), Malaysia were identified as a new species of *Chryseobacterium*, based on 16S rRNA sequencing, and taxonomically profiled as *C. artocarpi* CECT 8497 [15].

### 2.3. Characterisation and identification of the pigment

A loopful of bacterial isolate was cultured in 20 mL nutrient broth (in a 100 mL Erlenmeyer flask) and incubated at 30 °C, 200 rpm for 24 h. 10 mL of the active culture was transferred to 90 mL nutrient broth (in a 500 mL Erlenmeyer flask) and incubated as before. The culture broth (100 mL) was centrifuged at 10,000 rpm for 10 min and the resulting cell pellet was extracted using 10 mL of acetone [16]. The mixture of cell pellet and acetone was treated by ultrasonication for 2 min to bleach the cells completely and centrifuged at 8000 rpm for 5 min. The supernatant, containing the concentrated pigment, was collected and air dried, and the dry weight of the pigment was determined (7.214 mg/100 mL).

For pigment identification, the concentrated pigment was separated by column chromatography and analysed using NMR spectroscopy for $^{1}H$ (400 MHz) and $^{13}C$ (100 MHz), using a Bruker Avance 400 NMR spectrometer. The maximum wavelength, $\lambda_{max}$, of the purified pigment was determined using a UV–Vis spectrophotometer (PerkinElmer Lambda 950) between 800 and 200 nm. The pigment was purified further by liquid chromatography (reverse phase column-C18, methanol: water (75:25) as mobile phase) following the method of Rettori and Duran [17] and analysed by mass spectrometry (using electronspray ionisation as the ion source).

### 2.4. Synthesis of silver nanoparticles

10 mL of $AgNO_3$ ($10^{-3}$ M) solution was treated with 1 mL of flexirubin (in acetone) produced by *C. artocarpi* CECT 8497 and incubated at room temperature for 30 min. Over time, chemical reactions between the pigment and aqueous $AgNO_3$ caused the solution to turn brown in colour, indicating the formation of nanoparticles.

### 2.5. Characterisation of silver nanoparticles

#### 2.5.1. UV–Vis spectroscopy

The synthesis of flexirubin-mediated silver nanoparticles was confirmed initially by UV–Vis spectrometry (PerkinElmer Lambda 950), an important technique for verifying the formation of silver nanoparticles [4]. The UV–Vis spectra were obtained over a period of 15 min in the range 300 to 700 nm.

#### 2.5.2. Scanning electron microscopy (SEM) and energy dispersive X-ray spectroscopy (EDX)

SEM analysis (JSM-6460 LV) was performed at an accelerating voltage of 10 kV. The sample was prepared by dropping a very small amount of the sample onto a carbon coated copper grid and using blotting paper to remove excess solution. The film was allowed to dry under a mercury lamp for 5 min and before analysis. For EDX, the sample was dried and drop-coated onto a carbon film before analysis (Oxford Instrument, Thermo EDX, attached to SEM).

#### 2.5.3. X-ray diffraction (XRD)

The flexirubin-mediated silver nanoparticle solution was subjected to lyophilisation and powdered for XRD analysis. The XRD analysis was carried out by X-ray diffraction (Model D8, Bruker AXZ, Germany) at a voltage of 40 kV and a current of 40 mA using Cu-Kα radiation in the 2θ scan range of 20–80°. The average grain size of the silver nanoparticles was determined using the Debye–Scherrer equation.

#### 2.5.4. Fourier transform infrared (FTIR) spectroscopy

FTIR spectroscopy was performed to identify the functional groups capped on the surface of nanoparticles. For FTIR analysis, the flexirubin-mediated silver nanoparticle solution was centrifuged at 12,000 rpm for 30 min. The resulting pellet was washed three times with 25 mL of de-ionised water to remove any unattached biological moieties from the surface of the nanoparticles. The resulting residue was dried and ground with KBr, and spectra were obtained in the range of 400–4000 $cm^{-1}$ (Perkin Elmer, USA). FTIR of flexirubin was also performed to determine the possible reducing agent.

### 2.6. Anticancer activity

The MCF-7 human breast cancer cell line was obtained from the National Centre for Cell Sciences (NCCS), Pune, India. The cells were maintained in DMEM supplemented with 10% FBS, 1% L-glutamine, and 1% penicillin and streptomycin, and cultured in a 96 well plate at a density of $5 \times 10^3$ cells per well in a humidified $CO_2$ incubator at 37 °C for 24 h. Stock solutions of flexirubin and synthesised silver nanoparticles were prepared in sterile distilled water and diluted to the required concentrations using the cell culture medium. Cultured cell plates were treated with flexirubin (100 μg), silver nanoparticles (100 μg), flexirubin-mediated silver nanoparticles (100 μg) and incubated for a further 24 h at 37 °C. Non-treated cells were used as a control. Following incubation, 20 μL of MTT was added to each well and plates were incubated for 3 h. The medium was removed and the resulting formazan crystals were dissolved using 100 μL of DMSO before absorbance at 590 nm was measured in a microplate reader. The percentage of cell inhibition was calculated as follows:

$$\text{Cell inhibition}\,(\%) = \frac{\text{Absorption of the control} - \text{Absorption of the test}}{\text{Absorption of the control}} \times 100. \quad (1)$$

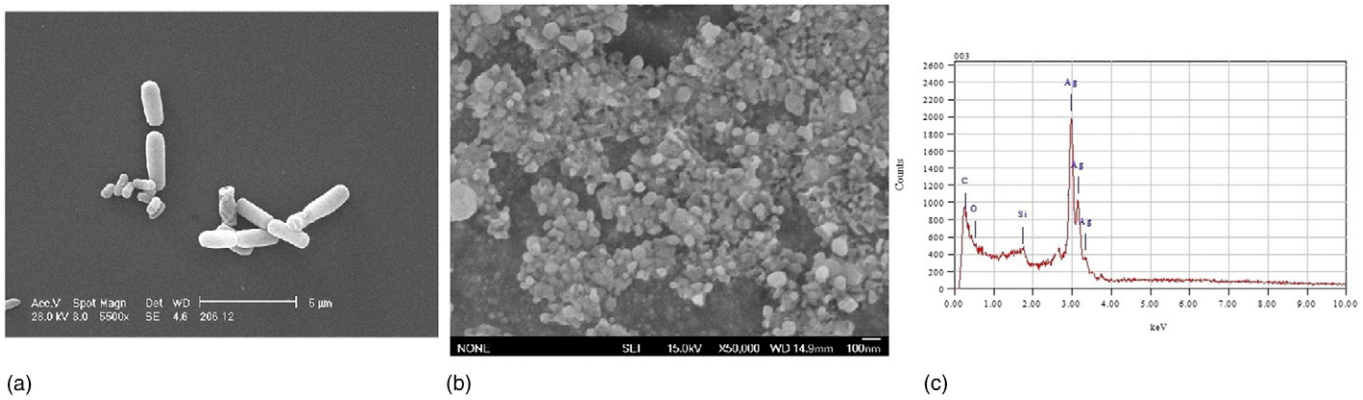


**Fig. 1.** (a) Scanning electron micrograph of *C. artocarpi* CECT 8497 grown on nutrient agar medium for 24 h at 30 °C. (b) FESEM image. (c) EDX micrograph of flexirubin mediated silver nanoparticles.

Furthermore, apoptosis in MCF-7 cells was assessed using fluorescent propidium iodide staining. The MCF-7 cells ($1 \times 10^6$ cells per well) were seeded in a 24 well plate and incubated until 90% confluent. Following treatment with flexirubin, silver nanoparticles, flexirubin-mediated silver nanoparticles at various concentrations for 24 h, cells were washed with ice cold PBS and fixed with 70% ethanol for 30 min. The plates were rinsed with ice cold PBS and stained with propidium iodide (500 μM) for 30 min. Nuclear staining of apoptotic cells (red colour) was observed by fluorescent microscopy (Nikon Eclipse, Japan). Each experiment was performed in duplicate.

## 3. Results and discussion

### 3.1. Characterisation of the isolate

The bacterial isolate formed yellowish orange, circular colonies on nutrient agar at 30 °C. Cells were determined as aerobic, Gram-negative, non-spore forming and non-motile rods (Fig. 1a). From the phylogenetic analysis, the strain fell into phylogenetic clus ters within the taxonomic variation encompassed by the genus *Chryseobacterium* and was taxonomically profiled as *C. artocarpi* CECT 8497 [15].

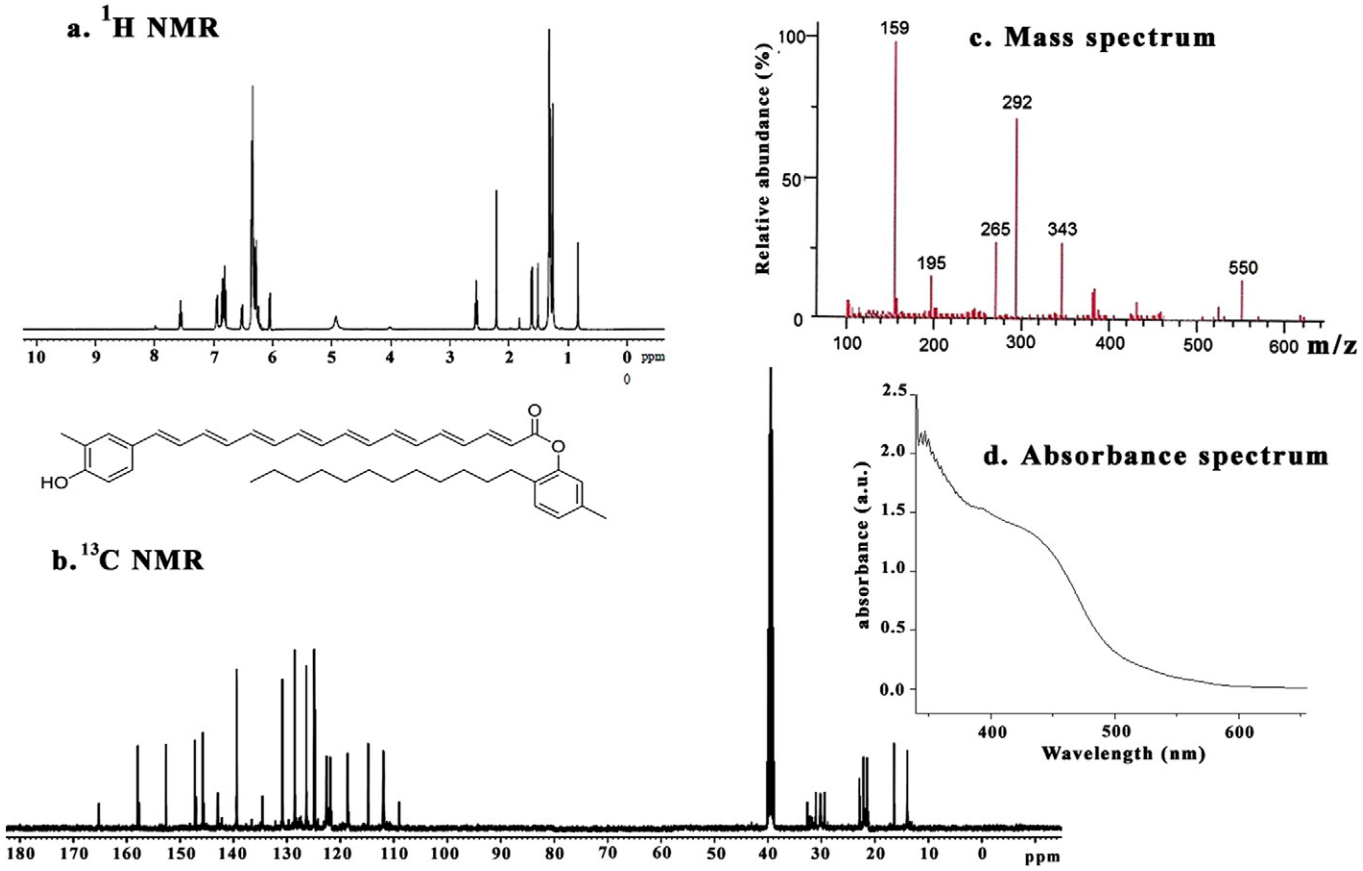


**Fig. 2.** (a) $^{1}$H NMR, (b) $^{13}$C NMR, (c) Mass spectrum, (d) UV–visible spectrum of pigment (flexirubin) produced by *C. artocarpi* CECT 8497.

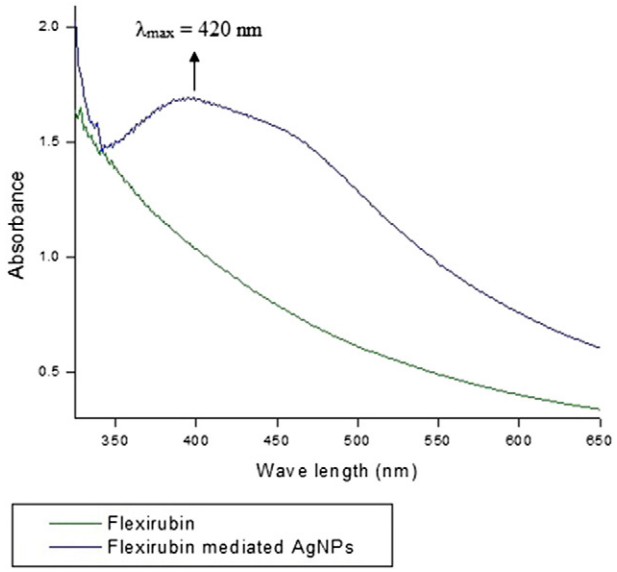


**Fig. 3.** UV–visible spectrum of flexirubin mediated silver nanoparticles.

### 3.2. Identification of the pigment

The $^{1}H$ NMR and $^{13}C$ NMR spectra of purified orange pigment are shown in Fig. 2a and b with resonances were completely assigned. The $^{1}H$ NMR spectrum represents the peaks corresponding to chemical shifts (54 protons) and the $^{13}C$ NMR spectrum displayed signals that correspond to aliphatic carbons as well as ethylene and aromatic carbons.

The yellowish-orange pigment was characterised by peak absorption between 400 and 450 nm and the mass spectrum exhibited a major peak at 159 nm, typical of a flexirubin-type pigment [13]. Flexirubin exhibits a characteristic mass spectrometric fragmentation pattern enabling the identification of a member of this class of compounds and substantial associated structural information (Fig. 2c, d). Mass spectrometry yielded the elementary composition $C_{43}H_{54}O_4$ and the electronic spectrum corresponded to that of an ω-phenyloctaenecarboxylic acid [18,19], suggesting a structural function, given that flexirubin functions as a photoprotective compound [20].

### 3.3. Synthesis and characterisation of silver nanoparticles

Since bacterial pigment was used in the synthesis of nanoparticles, there was no opportunity for contamination and the process was green. The synthesis of silver nanoparticles was initially confirmed by colour change in the reaction mixture and was due to the excitation of surface plasmon resonance (SPR) by the reduction of silver nitrate. A yield of approximately 0.17 g/100 mL was obtained from the synthetic process and used for further study. Manikprabhu and Lingappa [4] previously reported the synthesis of silver nanoparticles using *Streptomyces coelicolor* KLMP33 pigment with a yield of 0.14 g/100 mL. Flexirubins are a unique type of bacterial pigment, used in the treatment of chronic skin diseases, eczema, and gastric ulcers, etc. [21]. However, previous research on flexirubin is somewhat limited and the synthesis of silver nanoparticles was thus undertaken due to the unique properties of this pigment.

#### 3.3.1. UV–Vis spectroscopy

Fig. 3 illustrates an absorption peak around 420 nm, suggesting the presence of typical silver surface plasmon resonance [22]. It was shown that the active compound present in flexirubin had the ability to reduce silver nitrate. The colour intensity increased with reaction time and, following reduction, no further colour change was observed, indicating nanoparticle stability. The change in colour directly correlated with concentration and temperature, which may be due to the presence of reducing agents [9,23].

#### 3.3.2. Scanning electron microscopy–energy dispersive X-ray spectroscopy (SEM–EDX)

Fig. 1b shows the surface morphology of flexirubin-mediated silver nanoparticles. The image shows the synthesised silver nanoparticles having a spherical shape as well as some irregular shapes, indicating the stabilisation of nanoparticles by capping agents. The size of the synthesised particles was found to be approximately 49 nm. EDX analysis showed that silver was the major constituent element (Fig. 1c). The spectrum at 3 KeV indicated a strong signal for silver, characteristic of nano-sized metallic silver [12,24]. In addition, other peaks such as carbon and oxygen were observed due to unreacted precursors of $AgNO_3$ [25,26]. The silicon (Si) signal may be related to the glass slide used in the EDX analysis.

#### 3.3.3. X-ray diffraction (XRD)

The crystalline nature of the silver nanoparticles was determined by X-ray diffraction. Intense peaks corresponding to (111), (200), (220) and (311) were observed (Fig. 4). The peak at 28.5 may indicate the presence of the flexirubin complex along with nanoparticles. These peaks were indexed on the face centred cubic structure of metallic silver (JCPDS), confirming the crystalline nature of silver nanoparticles. The average crystallite size of the silver nanoparticles was determined using Scherer's equation (Eq. (2)):

$$D = \frac{K\lambda}{\beta \cos\theta} \tag{2}$$

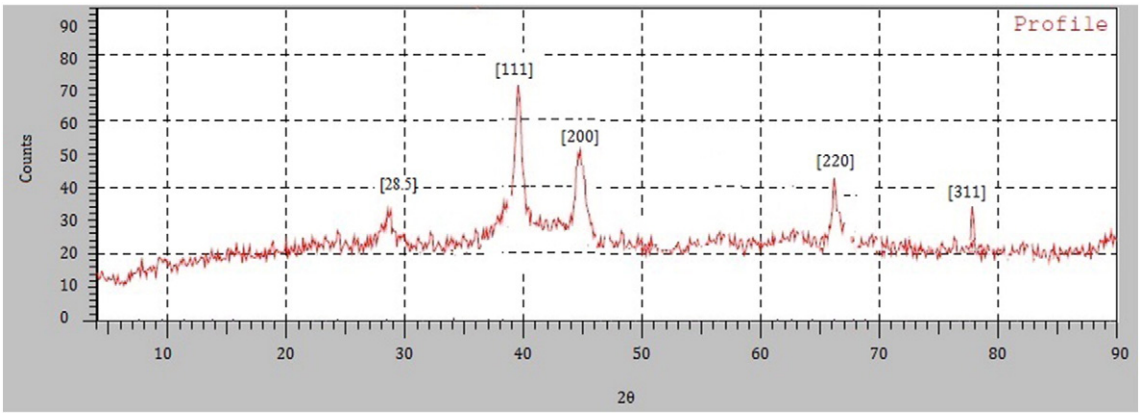


**Fig. 4.** XRD pattern of flexirubin mediated silver nanoparticles.

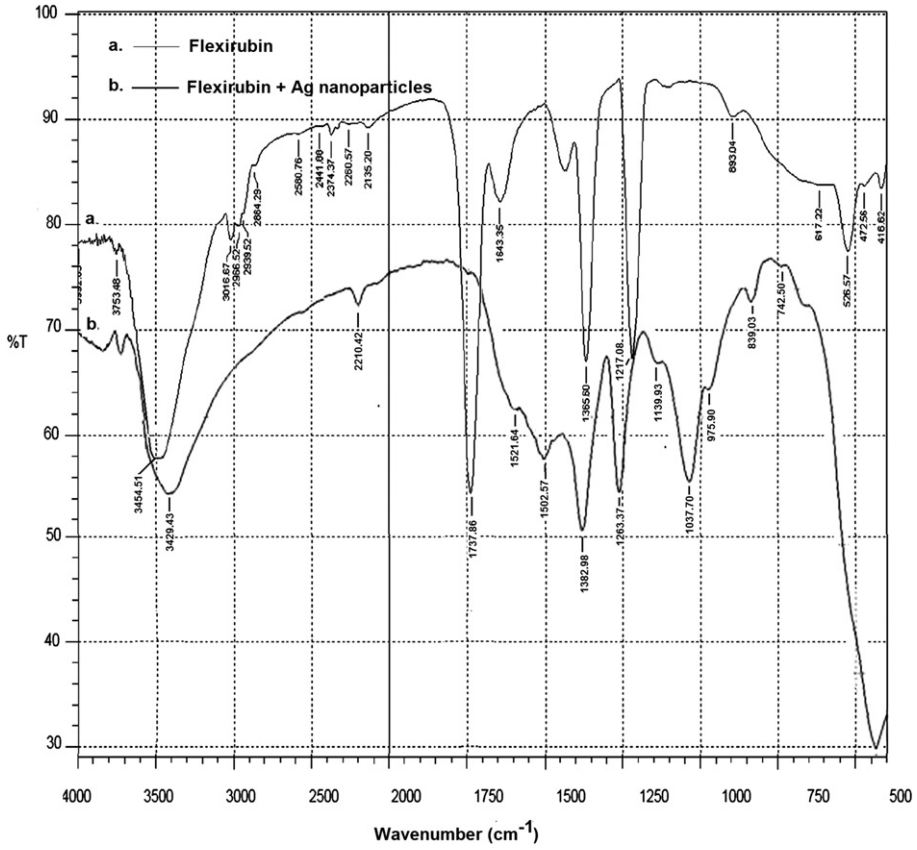


**Fig. 5.** FTIR spectrum of (a) flexirubin and (b) flexirubin mediated silver nanoparticles.

where 'D' is the crystallite size, 'K' is constant, λ is the wavelength of the X-ray source (0.154 nm), β is full width half maximum (FWHM), and θ is the diffraction angle. The calculated value for the flexirubin-mediated silver crystallite size was found to be approximately 42 nm.

### 3.3.4. Fourier transform infrared (FTIR) spectroscopy

Fig. 5 illustrate the FTIR spectra of the flexirubin and flexirubin-mediated silver nanoparticles. FTIR study of flexirubin alone produced absorption bands at 3454 $cm^{-1}$ assigned to O–H stretching, 1737 and 1643 $cm^{-1}$ assigned to asymmetrical and symmetrical stretching of the C = O group, and 1365 $cm^{-1}$ assigned to ester C–O group. The additional peaks at 1217 were assigned to the alkyl C–H stretching frequencies. FTIR study of flexirubin-mediated silver nanoparticles revealed intense absorption bands at 3429, 1521, 1502, 1382, 1263, and 1037 $cm^{-1}$ (Fig. 5b). It was observed that the absorption peaks at 3429, 1382, 1263 and 1037 $cm^{-1}$ represented the O–H, C–O, and alkyl C–H stretching frequencies. However, the asymmetrical and symmetrical stretching frequencies of the C═O group shifted at 1521 and

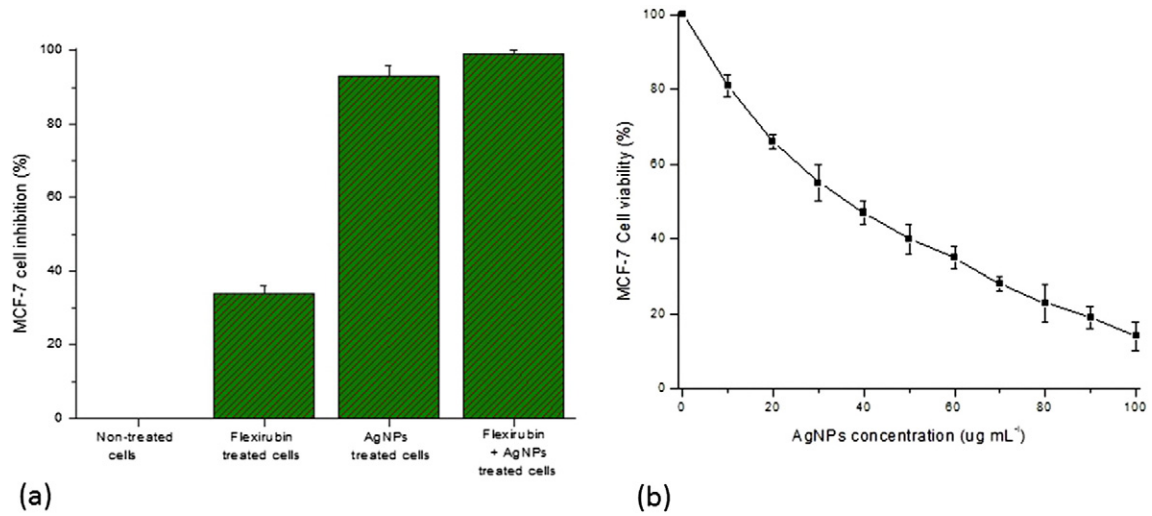


**Fig. 6.** (a) Anticancer activity of flexirubin (100 μg), silver nanoparticles (100 μg) and flexirubin mediated silver nanoparticles (100 μg) and (b) anticancer activity of silver nanoparticles at various concentrations against MCF-7 cells.

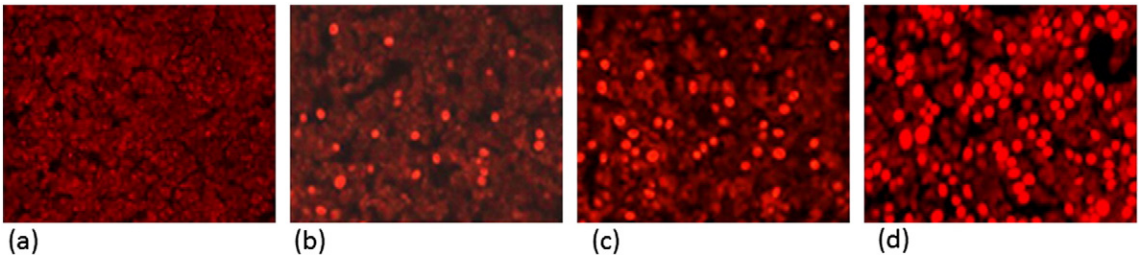


**Fig. 7.** Propidium iodide staining of MCF-7 cells. (a) Non-treated, (b) flexirubin (100 μg), (c) silver nanoparticles (100 μg) and (d) flexirubin mediated silver nanoparticles (100 μg) treated cells after 24 h.

1502 $cm^{-1}$ due to strong chelation of the ester carbonyl group of flexirubin with silver nanoparticles. The new absorption peak at 448 $cm^{-1}$ is a characteristic peak of silver nanoparticle–O═C bond formation [27]. Based on these observation, the following mechanism was proposed:

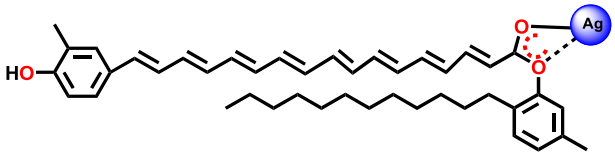


### 3.4. Anticancer activity

Anticancer properties of flexirubin and silver nanoparticles were investigated in a human breast cancer cell line (MCF-7). Fig. 6a illustrates the anticancer efficiency of flexirubin, silver nanoparticles, and flexirubin-mediated silver nanoparticles, found to be 34, 93, and 99%, respectively. These results clearly indicate that flexirubin and flexirubin-mediated silver nanoparticles may have potential as inhibitors of cancer cell growth. Furthermore, Fig. 6b shows that apoptosis in MCF-7 cells increased dose-wise with exposure to silver nanoparticle solution. The $IC_{50}$ value of the flexirubin-mediated silver nanoparticles was calculated as 36 μg $mL^{-1}$ and the silver nanoparticles inhibited 93% of cells at a concentration of 100 μg $mL^{-1}$. Fig. 7 shows the apoptotic cells stained with propidium iodide. Cells treated with flexirubin (100 μg), silver nanoparticles (100 μg), and flexirubin-mediated silver nanoparticles (100 μg) showed increased numbers of apoptotic cells. A higher number of apoptotic cells was observed in cells treated with flexirubin-mediated silver nanoparticles than in cells treated with flexirubin or silver nanoparticles alone. Various factors including composition, size, shape, surface charge, and capping molecules are known to affect the cytotoxicity of nanoparticles [28,29].

Treatment of a human cancer cell line with silver nanoparticles has been reported to initiate cell cycle arrest in the G2/M phase, possibly due to DNA damage. The silver nanoparticles directly modulated mitochondrial toxicity and DNA damage [30]. According to Asharani et al. [8], DNA damage was augmented by deposition, followed by the interaction of silver nanoparticles with DNA leading to cell cycle arrest in the G2/M phase. Biocompatible nature of flexirubin facilitates the entry of silver nanoparticles into the cell/nucleus potentially masking the silver nanoparticles during entry. This would increase the intake of silver leading to higher cell death. Moreover, the combination of silver and flexirubin may exert a synergistic cytotoxic effect on cancer cells. This work reports, for the first time, the synthesis of silver nanoparticles using flexirubin with subsequent potent anticancer properties.

## 4. Conclusion

Potent microbes are well-equipped to withstand metal stress in a nutrient-rich environment. We have isolated a novel *C. artocarpi* CECT 8497 flexirubin-producing bacterium and investigated its capability to synthesise silver nanoparticles. The nanoparticles were characterised by UV–Vis, XRD, SEM–EDX and FTIR methodologies. The synthesised silver nanoparticles had a spherical as well as some irregular shapes and the crystallite size was approximately 42 nm. The anticancer properties of flexirubin-mediated silver nanoparticles in a human breast cancer cell line were evaluated and found to inhibit 99% of the cells. The novelty of this approach includes the possibility of obtaining stable silver nanoparticles with potent anticancer activity in an eco-friendly manner. This study suggests that flexirubin-mediated silver nanoparticles may have potential as novel chemotherapeutic agents, thus advancing the future prospects of nanotechnology in the pharmaceutical industry.

## Acknowledgements

The authors are thankful to the Universiti Teknologi Malaysia for the Post-Doctoral Fellowship to Dr. C.K. Venil and Dr. P. Sathishkumar. The authors would like to thank the Research University grants (Q.J.130000.2526.07H03, Q.J.130000.2526.10J38, R.J.130000.7826.4F454), Ministry of Agriculture, Malaysia for the Technofund grant (TF0310F080) for financial support of research activities.

## References

[1] B. Ashe. M.Sc Thesis (2011) National Institute of Technology, India.
[2] Y.J. Song, H.K. Jang, B.S. Kim, Process Biochem. 44 (2009) 1133–1138.
[3] K. Sahayaraj, S. Rajesh, in: Mendez-Vilas Formatex (Ed.), Science Against Microbial Pathogens: Communicating Current Research and Technological Advances 2011, pp. 228–244 (Spain).
[4] D. Manikprabhu, K. Lingappa, Mater. Sci. Eng. C 45 (2014) 434–437.
[5] S. Verma, S. Abirami, V. Mahalakshmi, J. Microbiol. Biotech. Res. 3 (2013) 54–71.
[6] J.S. Kim, E. Kuk, K.N. Yu, J.H. Kim, S.J. Park, H.J. Lee, S.H. Kim, Y.K. Park, Y.H. Park, C.Y. Hwang, Y.K. Kim, Y.S. Lee, D.H. Jeong, M.H. Cho, Nanomed. Nanotechnol. Biol. Med. (3) (2007) 95–101.
[7] S. Sivamani, S. Jyothi, B. Joseph, B. Gunalan, B. Venkatesh, B. Kar, Int. J. Nanosci Nonotechnol. 4 (2013) 9–17.
[8] P.V. Asharani, M.P. Hande, S. Valiyaveettil, BMC Cell Biol. 10 (2009) 65.
[9] K. Vasanth, K. Ilango, R. Mohankumar, A. Agarwal, G.P. Dubey, Colloids Surf. B: Biointerfaces 117 (2014) 354–359.
[10] K. Sahayaraj, S. Rajesh, J.M. Rathi, Digest J. Nanomater. Biostruct. 7 (2012) 1557–1567.
[11] S. Iravani, Green Chem. 13 (2011) 2638–2650.
[12] P. Sivalingam, J.J. Antony, D. Siva, S. Achiraman, K. Anbarasu, Colloids Surf. B: Biointerfaces 98 (2012) 12–17.
[13] A. Bej. Patent PCT/US2010/024823/W) 2010096719 A2.
[14] J.S. Shim, J.O. Liu, Int. J. Biol. Sci. 10 (2014) 654–663.
[15] C.K. Venil, N. Nordin, Z.A. Zakaria, W.A. Ahmad, Int. J. Syst. Evol. Microbiol. 64 (2014) 3153–3159.
[16] R.P. Williams, J.A. Green, D.A. Rappoport, J. Bacteriol. 71 (1956) 115.
[17] D. Rettori, N. Duran, World J. Microbiol. Biotechnol. 14 (1998) 685–688.
[18] H. Reichenbach, H. Kleinig, Arch. Microbiol. 101 (1974) 134–144.
[19] M.H. Stafsnes, P. Bruheim, Book Chapter: Pigmented Marine Heterotrophic Bacteria: Occurrence, Diversity, and Characterization of Pigmentation, 2013 117–148.
[20] H. Irschik, H. Reichenbach, Biochim. Biophys. Acta Biomembr. 510 (1978) 1–10.
[21] S.K. Kim, Marine Biomaterials, CRC Press, Taylor & Francis, 2013.
[22] V.K. Vidhu, S.S. Aromal, D. Philip, Spectrochim. Acta A 83 (2011) 392–397.
[23] V. Karthick, V. Ganesh Kumar, T. Maiyalagan, R. Deepa, K. Govindaraju, A. Rajeswari, T.S. Dhas, Micro Nanosyst. 4 (2012) 192–198.
[24] P. Magudapathy, P. Gangopadhyay, B.K. Panigrahi, K.G.M. Nair, S. Dhara, Physica B 299 (2001) 142–146.
[25] V. Kathiravan, S. Ravi, S. Ashokkumar, Spectrochim. Acta A 130 (2014) 116–121.

[26] N. Kanipandian, S. Kannan, R. Ramesh, P. Subramaian, R. Thirumurugan, Mater. Res. Bull. 49 (2014) 494–502.
[27] K. Shameli, M.B. Ahmad, E.A.J. Al-Mulla, N.A. Ibrahim, P. Shabanzadeh, A. Rustaiyan, Y. Abdollahi, S. Bagheri, S. Abdolmohammadi, M.S. Usman, M. Zidan, Molecules 17 (2012) 8506–8517.
[28] E.E. Emekaa, O.C. Ojiefoh, C. Aleruchi, L.A. Hassan, O.M. Christiana, M. Rebecca, E.O. Darea, A.E. Temitope, Micron 57 (2014) 1–5.
[29] A.K. Suresh, D. Pelletier, W. Wang, J.L. Morrell-Falvey, B. Gu, M.J. Doktycz, Langmuir 28 (2012) 2727–2735.
[30] A.A. Kajani, A.K. Bordbar, S.H.Z. Esfahani, A.R. Khosropour, A. Razmjou, RSC Adv. 4 (2014) 61394–61403.